Smart Structures and Systems, *Vol. 25, No. 6* (*2020*) *707-717*
DOI: https://doi.org/10.12989/sss.2020.25.6.707

Nonlinear stability of smart nonlocal magneto-electro-thermo-elastic beams with geometric imperfection and piezoelectric phase effects

Nadhim M. Faleh*, Izz Kadhum Abboud and Amer Fadhel Nori

Al-Mustansiriah University, *Engineering Collage P.O. Box 46049*, *Bab-Muadum*, *Baghdad 10001*, *Iraq*

(*Received September 22, 2019, Revised December 1, 2019, Accepted January 15, 2020*)

Abstract. In this paper, analysis of thermal post-buckling behaviors of sandwich nanobeams with two layers of multi-phase magneto-electro-thermo-elastic (METE) composites have been presented considering geometric imperfection effects. Multi-phase METE material is composed form piezoelectric and piezo-magnetic constituents for which the material properties can be controlled based on the percentages of the constituents. Nonlinear governing equations of sandwich nanobeam are derived based on nonlocal elasticity theory together with classic thin beam model and an analytical solution is provided. It will be shown that post-buckling behaviors of sandwich nanobeam in thermo-electro-magnetic field depend on the constituent's percentages. Buckling temperature of sandwich nanobeam is also affected by nonlocal scale factor, magnetic field intensity and electrical voltage.

Keywords: sandwich nanobeam; multi-phase composite; thermal post-buckling; piezoelectric reinforcement; nonlocal elasticity

1. Introduction

Among different types of smart materials, the multi phases one known as magneto-electro-elastic (MEE) material represents superb possible application in smart structures/systems and also nano-sized devices owning to giving wonderful mechanical, electrical and magnetic coupling performances (Allam *et al*. 2018). Applying electro-magnetic fields to MEE nano-dimension beams yields elastic 2deformations and changed vibrational properties. Due to the reason that performing experiment on MEE nano-dimension beams are effortful yet, many scholars have represented their theoretical models taking into account small scales influences. Employing nonlocal theory of elasticity (Eringen 1972), one may be able to incorporate the small scales influences in theoretical model of nano-dimension beams (Thai and Vo 2012, Eltaher *et al*. 2012, Zemri *et al*. 2015, Bounouara *et al*. 2016, Akbas 2016, Besseghier *et al*. 2017, Mouffoki *et al*. 2017, Mirjavadi *et al*. 2017a, b, 2018a, b, 2019(a-f), Azimi *et al*. 2017, 2018). The theory recommends a scale factor called nonlocal parameter for describing that the stress fields at nano scales have a nonlocal character (Barati 2017, Ahmed *et al*. 2019, Al-Maliki *et al*. 2019, Fenjan *et al*. 2019).

The multi phases composite constructed by piezoelectric and piezo-magnetic constituents exhibits magneto-electrical influences which are invisible in single phase piezoelectric and MEE constituents (Nan 1994). Giving topmost mechanical efficiency under electrical and magnetic fields, a magneto-electro-elastic (MEE) material may be defined as a species of smart material having different application in sensing apparatus, smart systems and structural components (Aboudi 2001, Pan and Han 2005). Exposing to an exterior mechanical loading, a MEE material is capable to render electrical-magnetic field sensing (Li and Shi 2009, Guo *et al*. 2016). Furthermore, under electro-magnetic fields, such material experiences elastic deformations. For example, $BaTiO_3$ and $CoFe_2O_4$ may be composed to each other for creating a composite of MEE materials. According to the percentages of the two constituents, it is feasible to define material properties of the composite such as elastic moduli and piezo-magnetic constants. It is shown by other authors that vibration frequency of MEE structures is sensitive to the percentage of piezoelectric phase and hence vibration behavior of MEE can be controlled by varying the material composition (Kumaravel *et al*. 2007, Annigeri *et al*. 2007). There are also some studies on different structures in the literature (Chaudhary *et al*. 2017, 2018, 2019a, b, Sahu *et al*. 2018, Nirwal *et al*. 2019, Singh *et al*. 2018, Singhal *et al*. 2018a, b, 2019a, b, Singhal and Chaudhary 2019, Behera and Kumari 2018).

Up to now, several articles have been published about vibrational study of MEE nanoscale beams based on nonlocal theory of elasticity and different beam theories. Using nonlocal theory, an investigation of low amplitude free vibrational characteristics of smart nano-size beam made of MEE material has been carried out by Ke and Wang (2014). In a research, Jandaghian and Rahmani (2016) represented linearly type free vibrational study of magneto-electrically loaded nano-size beams embedded on elastic substrates. Buckling charactristics of a nonlocal smart nanobeam under magneto-electric field have been researched by Li *et al*. (2016). They showed that nonlocal effect leads to smaller buckling loads for the nanobeam.

All of afore-mentioned studies just examined perfect or

*Corresponding author, Professor,
E-mail: dr.nadhim@uomustansiriyah.edu.iq

ISSN: 1738-1584 (Print), 1738-1991 (Online)

straight MEE nano-size beams neglecting geometric imperfections influences. Assuming straight beam structures results in inaccurate findings owing to the fact that geometric imperfections are obvious during production as well as mounting of a structure (Mohammadi *et al*. 2014, Li *et al*. 2018, Mu'tasim *et al*. 2017, Eshraghi *et al*. 2016, Mohammadimehr and Alimirzaei 2016). It has been stated that the buckling behaviors of nano-size beams are relied on the amplitude value of geometrical imperfections. According to this discussion, it may be concluded that it is important to incorporate geometric imperfection effects on buckling behaviors of nonlocal MEE nano-scale beams.

In this paper, analysis of thermal post-buckling behaviors of sandwich nanobeams with two layers of multi-phase magneto-electro-thermo-elastic (METE) composites have been presented considering geometric imperfection effects. Multi-phase METE material is composed form piezoelectric and piezo-magnetic constituents for which the material properties can be controlled based on the percentages of the constituents. Nonlinear governing equations of sandwich nanobeam are derived based on nonlocal elasticity theory together with classic thin beam model and an analytical solution is provided. It will be shown that post-buckling behaviors of sandwich nanobeam in electro-magnetic field depend on the constituent's percentages. Buckling temperature of sandwich nanobeam is also affected by nonlocal scale factor, magnetic field intensity and electrical voltage.

2. Magneto-electro-elastic composites with two phases

For two-phase METE composites, all material characteristics are associated with the portion (volume fraction) of piezoelectric constituent (V_f). In the present paper, the nanobeam is made of piezo-magnetic $BaTiO_3$-$CoFe_2O_4$ material and Table 1 represents material coefficients. In this material, $BaTiO_3$ is the piezoelectric constituent and then $CoFe_2O_4$ is the piezo-magnetic constituent. Table 1 respectively defines elastic (C_{ij}), piezoelectric (e_{ij}) and piezo-magnetic (q_{ij}) properties. Moreover, k_{ij}, d_{ij} and x_{ij} respectively denote dielectric, magnetic-electric-elastic and magnetic permeability properties.

3. Sandwich beams with two layers of multi-phase METE material

In order to develop nonlinear formulation for nonlinear buckling of nonlocal beam, well-known classical beam theory has been used in the present paper. Thus, the displacements of beam (u_1, $u_2 = 0$, u_3) may be written based on axial (u) and transverse (w) field variables as (Bensattalah *et al*. 2018)

$$u_1(x,y,z) = u(x,y) - z\frac{\partial w}{\partial x} \tag{1}$$

$$u_3(x,y,z) = w(x,y) \tag{2}$$

For the classic beam model, the strain field including geometric imperfection deflection (w^*) might be expressed by

$$\varepsilon_{xx} = \frac{\partial u_1}{\partial x} = \frac{\partial u}{\partial x} - z\frac{\partial^2 w}{\partial x^2} + \frac{1}{2}\left(\frac{\partial w}{\partial x}\right)^2 + \frac{\partial w}{\partial x}\frac{\partial w^*}{\partial x} \tag{3}$$

Table 2 Validation of buckling load of a perfect piezo-magnetic nanobeams

	ea = 0 nm	ea = 1 nm	ea = 2 nm	ea = 3 nm
Li *et al.* (2016)	0.8189	0.7198	0.5564	0.4089
Present	0.8189	0.7199	0.5564	0.4089

Table 1 Material properties of $BaTiO_3$-$CoFe_2O_4$ composites

Property	$V_f = 0$	$V_f = 0.2$	$V_f = 0.4$	$V_f = 0.6$	$V_f = 0.8$
C_{11} (GPa)	286	250	225	200	175
C_{13}	170	145	125	110	100
C_{33}	269.5	240	220	190	170
e_{31} (C/m^2)	0	-2	-3	-3.5	-4
e_{33}	0	4	7	11	14
q_{31} (N/Am)	580	410	300	200	100
q_{33}	700	550	380	260	120
k_{11} $(10^{-9}\ C/Vm)$	0.08	0.33	0.8	0.9	1
k_{33}	0.093	2.5	5	7.5	10
d_{11} $(10^{-12}\ Ns/VC)$	0	2.8	4.8	6	6.8
d_{33}	0	2000	2750	2500	1500
x_{11} $(10^{-4}\ Ns^2/C^2)$	-5.9	-3.9	-2.5	-1.5	-0.8
x_{33}	1.57	1.33	1	0.75	0.5
α_1 (10^{-6})	10	11.7	13	14.11	14.98
α_3	10	9.72	9.15	8.37	7.44

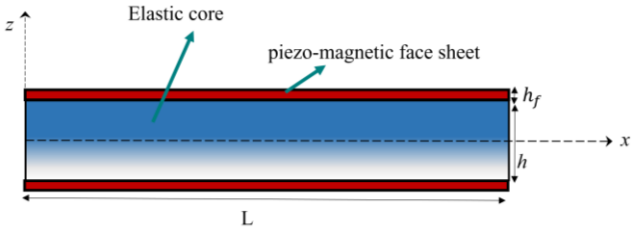

Fig. 1 Geometry of a sandwich nanobeam having three layers

Considering the fact that the sandwich nanobeam shown in Fig. 1 is under coupled electro-magnetic field with electrical potential (Φ) and magnetic potential (Υ), one can define the potentials in following forms as functions of electrical voltage (V_E) and magnetic potential intensity (Ω) as (Li *et al*. 2016)

$$\Phi(x,y,z) = -cos(\beta z)\phi(x,y) + \frac{2z}{h}V \tag{4}$$

$$\Upsilon(x,y,z) = -cos(\beta z)\gamma(x,y) + \frac{2z}{h}\Omega \tag{5}$$

with $\beta = \pi/h$. Calculating the two-dimensional gradient of electro-magnetic potentials gives the electrical field components (E_x, E_z) and magnet field components (H_x, H_z) as follows

$$\begin{aligned} E_x &= -\Phi_{,x} = cos(\beta z)\frac{\partial \phi}{\partial x}, \\ E_z &= -\Phi_{,z} = -\beta\, sin(\beta z)\phi - \frac{2V}{h} \end{aligned} \tag{6}$$

$$\begin{aligned} H_x &= -\Upsilon_{,x} = cos(\beta z)\frac{\partial \gamma}{\partial x}, \\ H_z &= -\Upsilon_{,z} = -\beta\, sin(\beta z)\gamma - \frac{2\Omega}{h} \end{aligned} \tag{7}$$

For a METE nano-size beam, the governing equations based on classic beam theory and nonlocal stress effects may be expressed by (Ke and Wang 2014)

$$\frac{\partial N_x}{\partial x} = 0 \tag{8}$$

$$\frac{\partial^2 M_x}{\partial x^2} + \frac{\partial}{\partial x}\left(N_x\left[\frac{\partial w}{\partial x} + \frac{\partial w^*}{\partial x}\right]\right) = 0 \tag{9}$$

$$\int_{-h/2}^{h/2}\left(cos(\beta z)\frac{\partial D_x}{\partial x} + \beta\, sin(\beta z)D_z\right)dz = 0 \tag{10}$$

$$\int_{-h/2}^{h/2}\left(cos(\beta z)\frac{\partial B_x}{\partial x} + \beta\, sin(\beta z)B_z\right)dz = 0 \tag{11}$$

in which D_i, B_i represent the components for electric and magnetic field displacements; k_L, k_P, K_{NL} are linear, shear and nonlinear layers of elastic substrate. Also, N_x and M_x are in-plane force and bending moment defined as

$$(N_x, M_x) = \int_A (1, z, f)\sigma_x\, dA \tag{12}$$

Also, the boundary conditions are

$$N_x = 0 \quad \text{or} \quad u = 0 \tag{13}$$

$$\frac{\partial M_x}{\partial x} + N_x\left[\frac{\partial w}{\partial x} + \frac{\partial w^*}{\partial x}\right] = 0 \quad \text{or} \quad w = 0 \tag{14}$$

$$\int_{-h/2}^{h/2} cos(\beta z)D_x dz = 0 \quad \text{or} \quad \phi = 0 \tag{15}$$

$$\int_{-h/2}^{h/2} cos(\beta z)B_x dz = 0 \quad \text{or} \quad \gamma = 0 \tag{16}$$

All ingredients of stress field, electrical field displacement (D_x, D_z) and magnetic induction (B_x, B_z) for a size-dependent beam relevant to nonlocal theory may be written as

$$\begin{aligned} &(1-(ea)^2\nabla^2)\sigma_{xx} \\ &= \tilde{c}_{11}(\varepsilon_{xx} - \tilde{\alpha}\Delta T) - \tilde{e}_{31}E_z - \tilde{q}_{31}H_z \end{aligned} \tag{17}$$

$$(1-(ea)^2\nabla^2)D_x = \tilde{e}_{15}\gamma_{xz} + \tilde{k}_{11}E_x + \tilde{d}_{11}H_x \tag{18}$$

$$(1-(ea)^2\nabla^2)D_z = \tilde{e}_{31}\varepsilon_{xx} + \tilde{k}_{33}E_z + \tilde{d}_{33}H_z \tag{19}$$

$$(1-(ea)^2\nabla^2)B_x = \tilde{q}_{15}\gamma_{xz} + \tilde{d}_{11}E_x + \tilde{\chi}_{11}H_x \tag{20}$$

$$(1-(ea)^2\nabla^2)B_z = \tilde{q}_{31}\varepsilon_{xx} + \tilde{d}_{33}E_z + \tilde{\chi}_{33}H_z \tag{21}$$

So that *ea* is nonlocal scale factor; Elastic, piezoelectric and magnetic material characteristics have been respectively marked by C_{ij}, e_{ij} and q_{ij}. For considering plane stress conditions, all material properties are expressed in a new form as follows (Ke and Wang 2014)

$$\begin{aligned} &\tilde{c}_{11} = c_{11} - \frac{c_{13}^2}{c_{33}}, \quad \tilde{c}_{12} = c_{12} - \frac{c_{13}^2}{c_{33}}, \quad \tilde{c}_{66} = c_{66}, \\ &\tilde{e}_{15} = e_{15}, \quad \tilde{e}_{31} = e_{31} - \frac{c_{13}e_{33}}{c_{33}}, \\ &\tilde{q}_{15} = q_{15}, \quad \tilde{q}_{31} = q_{31} - \frac{c_{13}q_{33}}{c_{33}}, \\ &\tilde{d}_{11} = \tilde{d}_{11}, \quad \tilde{d}_{33} = \tilde{d}_{33} + \frac{q_{33}e_{33}}{c_{33}}, \end{aligned} \tag{22}$$

$$\begin{aligned} &\tilde{k}_{11} = k_{11}, \quad \tilde{k}_{33} = k_{33} + \frac{e_{33}^2}{c_{33}}, \quad \tilde{\chi}_{11} = \chi_{11}, \\ &\tilde{\chi}_{33} = \chi_{33} + \frac{q_{33}^2}{c_{33}}, \quad \tilde{\alpha} = \alpha_1 - \frac{c_{13}\alpha_3}{c_{33}} \end{aligned} \tag{23}$$

By integration from Eqs. (17)-(21) over the total thickness of nano-size sandwich beam, the following resultants for a sandwich nanobeam would be derived

$$\begin{aligned} &(1-(ea)^2\nabla^2)N_x \\ &= A_{11}\left(\frac{\partial u}{\partial x} + \frac{1}{2}\left(\frac{\partial w}{\partial x}\right)^2 + \frac{\partial w}{\partial x}\frac{\partial w^*}{\partial x}\right) - B_{11}\frac{\partial^2 w}{\partial x^2} \\ &+A_{31}^e\phi + A_{31}^m\gamma - N_x^E - N_x^H - N_x^T \end{aligned} \tag{24}$$

$$(1-(ea)^2\nabla^2)M_x = B_{11}\left(\frac{\partial u}{\partial x}+\frac{1}{2}\left(\frac{\partial w}{\partial x}\right)^2+\frac{\partial w}{\partial x}\frac{\partial w^*}{\partial x}\right)-D_{11}\frac{\partial^2 w}{\partial x^2} +E_{31}^e\phi+E_{31}^m\gamma-M_x^E-M_x^H-M_x^T \tag{25}$$

$$\int_{-\frac{h}{2}}^{\frac{h}{2}}(1-(ea)^2\nabla^2)D_x\cos(\beta z)dz = F_{11}^e\frac{\partial\phi}{\partial x}+F_{11}^m\frac{\partial\gamma}{\partial x} \tag{26}$$

$$\int_{-\frac{h}{2}}^{\frac{h}{2}}(1-(ea)^2\nabla^2)D_z\beta\sin(\beta z)dz = A_{31}^e\left(\frac{\partial u}{\partial x}+\frac{1}{2}\left(\frac{\partial w}{\partial x}\right)^2+\frac{\partial w}{\partial x}\frac{\partial w^*}{\partial x}\right)-E_{31}^e\frac{\partial^2 w}{\partial x^2} -F_{33}^e\phi-F_{33}^m\gamma \tag{27}$$

$$\int_{-\frac{h}{2}}^{\frac{h}{2}}(1-(ea)^2\nabla^2)B_x\cos(\beta z)dz = +F_{11}^m\frac{\partial\phi}{\partial x}+X_{11}^m\frac{\partial\gamma}{\partial x} \tag{28}$$

$$\int_{-\frac{h}{2}}^{\frac{h}{2}}(1-(ea)^2\nabla^2)B_z\beta\sin(\beta z)dz = A_{31}^m\left(\frac{\partial u}{\partial x}+\frac{1}{2}\left(\frac{\partial w}{\partial x}\right)^2+\frac{\partial w}{\partial x}\frac{\partial w^*}{\partial x}\right) -E_{31}^m\nabla^2 w-F_{33}^m\phi-X_{33}^m\gamma \tag{29}$$

in which

$$\{A_{11},B_{11},D_{11}\}=\int_{-h/2}^{h/2}\tilde{c}_{11}(1,z,z^2)\,dz \tag{30}$$

$$\{A_{31}^e,E_{31}^e\}=\int_{-h/2}^{h/2}\tilde{e}_{31}\beta\sin(\beta z)\{1,z\}\,dz \tag{31}$$

$$\{A_{31}^m,E_{31}^m\}=\int_{-h/2}^{h/2}\tilde{q}_{31}\beta\sin(\beta z)\{1,z\}\,dz \tag{32}$$

$$\{F_{11}^e,F_{33}^e\}=\int_{-h/2}^{h/2}\left\{\tilde{k}_{11}\cos^2(\beta z),\tilde{k}_{33}\beta^2\sin^2(\beta z)\right\}dz \tag{33}$$

$$\{F_{11}^m,F_{33}^m\}=\int_{-h/2}^{h/2}\left\{\tilde{d}_{11}\cos^2(\beta z),\tilde{d}_{33}\beta^2\sin^2(\beta z)\right\}dz \tag{34}$$

$$\{X_{11}^m,X_{33}^m\}=\int_{-h/2}^{h/2}\{\tilde{\chi}_{11}\cos^2(\beta z),\tilde{\chi}_{33}\beta^2\sin^2(\beta z)\}\,dz \tag{35}$$

Moreover, electric, magnetic and thermal fields exerts in-plane loads and moments which exist in Eqs. (24)-(25) as

$$N_x^E=-\int_{-\frac{h}{2}}^{\frac{h}{2}}\tilde{e}_{31}\frac{2V}{h}dz,\quad N_x^H=-\int_{-\frac{h}{2}}^{\frac{h}{2}}\tilde{q}_{31}\frac{2\Omega}{h}dz, \quad N_x^T=\int_{-h/2}^{h/2}\tilde{\alpha}\tilde{c}_{11}\Delta T dz \tag{36}$$

$$M_x^E=-\int_{-\frac{h}{2}}^{\frac{h}{2}}\tilde{e}_{31}\frac{2V}{h}zdz,\quad M_x^H=-\int_{-\frac{h}{2}}^{\frac{h}{2}}\tilde{q}_{31}\frac{2\Omega}{h}zdz, \quad M_x^T=\int_{-h/2}^{h/2}\tilde{\alpha}\tilde{c}_{11}\Delta T z dz \tag{37}$$

The governing equations for a multi-phase nano-scale beam based upon displacement components would be obtained by inserting Eqs. (24)-(29), into Eqs. (8)-(11) as follows

$$A_{11}\left(\frac{\partial^2 u}{\partial x^2}+\frac{\partial w}{\partial x}\frac{\partial^2 w}{\partial x^2}+\frac{\partial^2 w}{\partial x^2}\frac{\partial w^*}{\partial x}+\frac{\partial w}{\partial x}\frac{\partial^2 w^*}{\partial x^2}\right) -B_{11}\frac{\partial^3 w}{\partial x^3}+A_{31}^e\frac{\partial\phi}{\partial x}+A_{31}^m\frac{\partial\gamma}{\partial x}=0 \tag{38}$$

$$-D_{11}\frac{\partial^4 w}{\partial x^4}+E_{31}^e\left(\frac{\partial^2\phi}{\partial x^2}\right)+E_{31}^m\left(\frac{\partial^2\gamma}{\partial x^2}\right) +(1-(ea)^2\nabla^2)\left(+\left(A_{11}\left(\frac{\partial u}{\partial x}+\frac{1}{2}\left(\frac{\partial w}{\partial x}\right)^2+\frac{\partial w}{\partial x}\frac{\partial w^*}{\partial x}\right)\right.\right. \left.\left.-B_{11}\frac{\partial^2 w}{\partial x^2}A_{31}^e\phi+A_{31}^m\gamma-N_x^E-N_x^H\right)\left[\frac{\partial^2 w}{\partial x^2}+\frac{\partial^2 w^*}{\partial x^2}\right] =0 \tag{39}$$

$$A_{31}^e\left(\frac{\partial u}{\partial x}+\frac{1}{2}\left(\frac{\partial w}{\partial x}\right)^2+\frac{\partial w}{\partial x}\frac{\partial w^*}{\partial x}\right)-E_{31}^e\left(\frac{\partial^2 w}{\partial x^2}\right) +F_{11}^e\left(\frac{\partial^2\phi}{\partial x^2}\right)+F_{11}^m\left(\frac{\partial^2\gamma}{\partial x^2}\right)-F_{33}^e\phi-F_{33}^m\gamma=0 \tag{40}$$

$$A_{31}^m\left(\frac{\partial u}{\partial x}+\frac{1}{2}\left(\frac{\partial w}{\partial x}\right)^2+\frac{\partial w}{\partial x}\frac{\partial w^*}{\partial x}\right)-E_{31}^m\left(\frac{\partial^2 w}{\partial x^2}\right) +F_{11}^m\left(\frac{\partial^2\phi}{\partial x^2}\right)+X_{11}^m\left(\frac{\partial^2\gamma}{\partial x^2}\right)-F_{33}^m\phi-X_{33}^m\gamma=0 \tag{41}$$

An important conclusion from Eq. (38) is

$$A_{11}\left(\frac{\partial u}{\partial x}+\frac{1}{2}\left(\frac{\partial w}{\partial x}\right)^2+\frac{\partial w}{\partial x}\frac{\partial w^*}{\partial x}\right)+A_{31}^e\phi+A_{31}^m\gamma -N_x^E-N_x^H-N_x^T=C_1 \tag{42}$$

Then

$$\frac{\partial u}{\partial x}=-\frac{1}{2}\left(\frac{\partial w}{\partial x}\right)^2-\frac{\partial w}{\partial x}\frac{\partial w^*}{\partial x}-\frac{A_{31}^e}{A_{11}}\phi -\frac{A_{31}^m}{A_{11}}\gamma+\frac{N_x^E}{A_{11}}+\frac{N_x^H}{A_{11}}+\frac{N_x^T}{A_{11}}+\frac{C_1}{A_{11}} \tag{43}$$

Now, integrating Eq. (43) yields

$$u=-\frac{1}{2}\int_0^x\left(\frac{\partial w}{\partial x}\right)^2dx-\int_0^x\frac{\partial w}{\partial x}\frac{\partial w^*}{\partial x}dx-\frac{A_{31}^e}{A_{11}}\int_0^x\phi\,dx -\frac{A_{31}^m}{A_{11}}\int_0^x\gamma\,dx+\frac{N_x^E}{A_{11}}\int_0^x dx+\frac{N_x^H}{A_{11}}\int_0^x dx +\frac{N_x^T}{A_{11}}\int_0^x dx+\frac{C_1}{A_{11}}x+C_2 \tag{44}$$

Next, by considering boundary conditions $u(0) = 0$, $u(L)$

= 0 the two constants would be obtained

$$C_2 = 0$$
$$C_1 = \frac{A_{11}}{2L}\int_0^L (\frac{\partial w}{\partial x})^2\,dx + \frac{A_{11}}{L}\int_0^L \frac{\partial w}{\partial x}\frac{\partial w^*}{\partial x}\,dx + \frac{A_{31}^e}{L}\int_0^L \phi\,dx + \frac{A_{31}^m}{L}\int_0^L \gamma\,dx - (N_x^E + N_x^H + N_x^T) \quad (45)$$

Now, obtained constant must be inserted into Eq. (44). Then, the governing equations reduce to

$$-D_{11}\frac{\partial^4 w}{\partial x^4} + E_{31}^e\left(\frac{\partial^2 \phi}{\partial x^2}\right) + E_{31}^m\left(\frac{\partial^2 \gamma}{\partial x^2}\right) + (1-(ea)^2\nabla^2)\left(+\left(A_{11} + \frac{1}{2L}\int_0^L \left(\frac{\partial w}{\partial x}\right)^2 dx + \frac{1}{L}\int_0^L \frac{\partial w}{\partial x}\frac{\partial w^*}{\partial x}dx\right) - B_{11}\frac{\partial^2 w}{\partial x^2} - N_x^E - N_x^H - N_x^T\right)\left[\frac{\partial^2 w}{\partial x^2} + \frac{\partial^2 w^*}{\partial x^2}\right]\right) = 0 \quad (46)$$

$$A_{31}^e\left(-\frac{A_{31}^e}{A_{11}}\phi - \frac{A_{31}^m}{A_{11}}\gamma + \frac{1}{2L}\int_0^L \left(\frac{\partial w}{\partial x}\right)^2 dx + \frac{1}{L}\int_0^L \frac{\partial w}{\partial x}\frac{\partial w^*}{\partial x}dx\right) - E_{31}^e\left(\frac{\partial^2 w}{\partial x^2}\right) + F_{11}^e\left(\frac{\partial^2 \phi}{\partial x^2}\right) + F_{11}^m\left(\frac{\partial^2 \gamma}{\partial x^2}\right) - F_{33}^e\phi - F_{33}^m\gamma = 0 \quad (47)$$

$$A_{31}^m\left(-\frac{A_{31}^e}{A_{11}}\phi - \frac{A_{31}^m}{A_{11}}\gamma + \frac{1}{2L}\int_0^L (\frac{\partial w}{\partial x})^2\,dx + \frac{1}{L}\int_0^L \frac{\partial w}{\partial x}\frac{\partial w^*}{\partial x}dx\right) - E_{31}^m\left(\frac{\partial^2 w}{\partial x^2}\right) + F_{11}^m\left(\frac{\partial^2 \phi}{\partial x^2}\right) + X_{11}^m\left(\frac{\partial^2 \gamma}{\partial x^2}\right) - F_{33}^m\phi - X_{33}^m\gamma = 0 \quad (48)$$

4. Method of solution

The governing equation for sandwich nano-size beam only contains three displacements which need to be approximated based on following assumption (Barati 2017)

$$w = \sum_{i=1}^{\infty} \widetilde{W}_m X_i(x) \quad (49)$$

$$\phi = \sum_{i=1}^{\infty} \Phi_m X_i(x) \quad (50)$$

$$\gamma = \sum_{i=1}^{\infty} \Upsilon_m X_i(x) \quad (51)$$

where (W_m ,Φ_m, Υ_m) are the unknown coefficients and the function X_m defines a trial function for considering boundary conditions; $X_i = 0.5(1 - cos(2i\pi x/L))$ for clamped-clamped conditions. Then, the imperfection shape is considered as first buckling mode of the nano-size beam as

$$w^* = \sum_{i=1}^{\infty} W^* F_i(x) \quad (52)$$

in which W^* defines the imperfections amplitude and F_i defines the shape functions for imperfections. Placing Eqs. (49)-(52) into Eqs. (46)-(48) gives three equations as

$$\begin{aligned} &K_1^S\widetilde{W} + G_1\widetilde{W}^3 + Q_1\widetilde{W}^2 + K_1^E\Phi_m + K_1^H\Upsilon_m + \Psi_1 W^* = 0 \\ &K_2^S\widetilde{W} + G_2\widetilde{W}^2 + K_2^E\Phi_m + K_2^H\Upsilon_m = 0 \\ &K_3^S\widetilde{W} + G_3\widetilde{W}^2 + K_3^E\Phi_m + K_3^H\Upsilon_m = 0 \end{aligned} \quad (53)$$

in which

$$K_1^S = -D_{11}(\Lambda_{40}) - (N_x^E + N_x^H + N_x^T)\Lambda_{20} + (ea)^2(N_x^E + N_x^H + N_x^T)\Lambda_{40} + \frac{A_{11}}{L}\Xi_{11}\Gamma_{20}W^{*2} - (ea)^2\frac{A_{11}}{L}\Xi_{11}\Gamma_{40}W^{*2} \quad (54)$$

$$G_1 = \frac{A_{11}}{2L}\Lambda_{11}\Lambda_{20} - (ea)^2\frac{A_{11}}{2L}\Lambda_{11}\Lambda_{40} \quad (55)$$

$$Q_1 = \frac{A_{11}}{2L}\Lambda_{11}\Gamma_{20}W^* - (ea)^2\frac{A_{11}}{2L}\Lambda_{11}\Gamma_{40}W^* + \frac{A_{11}}{L}\Xi_{11}\Lambda_{20}W^* - (ea)^2\frac{A_{11}}{L}\Xi_{11}\Lambda_{40}W^* \quad (56)$$

$$K_1^E = E_{31}^e\Lambda_{20} \quad (56)$$

$$K_1^H = E_{31}^m\Lambda_{20} \quad (57)$$

$$K_2^S = -E_{31}^e\Lambda_{20} + \frac{A_{31}^e}{L}\Lambda_0\Xi_{11}W^* \quad (58)$$

$$K_3^S = -E_{31}^m\Lambda_{20} + \frac{A_{31}^m}{L}\Lambda_0\Xi_{11}W^* \quad (59)$$

$$G_2 = \frac{A_{31}^e}{2L}\Lambda_0\Lambda_{11} \quad (60)$$

$$G_3 = \frac{A_{31}^m}{2L}\Lambda_0\Lambda_{11} \quad (61)$$

$$K_2^E = -\frac{(A_{31}^e)^2}{A_{11}}\Lambda_{00} + F_{11}^e\Lambda_{20} - F_{33}^e\Lambda_{00} \quad (62)$$

$$K_2^H = -\frac{A_{31}^eA_{31}^m}{A_{11}}\Lambda_{00} + F_{11}^m\Lambda_{20} - F_{33}^m\Lambda_{00} \quad (63)$$

$$K_3^E = -\frac{A_{31}^eA_{31}^m}{A_{11}}\Lambda_{00} + F_{11}^m\Lambda_{20} - F_{33}^m\Lambda_{00} \quad (64)$$

$$K_3^H = -\frac{(A_{31}^m)^2}{A_{11}}\Lambda_{00} + X_{11}^m\Lambda_{20} - X_{33}^m\Lambda_{00} \quad (65)$$

$$\Psi_1 = -(N_x^E + N_x^H + N_x^T)\Gamma_{20} + (ea)^2(N_x^E + N_x^H + N_x^T)\Gamma_{40} \quad (66)$$

where

$$\Lambda_{00}=\int_0^L X_iX_i dx\,,\quad \Lambda_{20}=\int_0^L X_i^{''}X_i dx$$
$$\Lambda_{40}=\int_0^L X_i^{''''}X_i dx\,,\quad \Lambda_{11}=\int_0^L X_i^{'}X_i^{'} dx$$
$$\Xi_{11}=\int_0^L F_i^{'}X_i^{'} dx \qquad (67)$$
$$\Gamma_{20}=\int_0^L F_i^{''}F_i dx,\quad \Gamma_{40}=\int_0^L F_i^{''''}F_i dx$$

By using last two relations of Eq. (53), one may derive the unknowns Φ_m and Υ_m as follows

$$\Phi_m=Z_1\widetilde{W}+Z_2\widetilde{W}^2,\qquad \Upsilon_m=Z_3\widetilde{W}+Z_4\widetilde{W}^2$$
$$Z_1=-\frac{(K_2^HK_3^S-K_3^HK_2^S)}{K_3^EK_2^H-K_2^EK_3^H},\quad Z_2=-\frac{(G_3K_2^H-G_2K_3^H)}{K_3^EK_2^H-K_2^EK_3^H} \qquad (68)$$
$$Z_3=-\frac{(K_3^EK_2^S-K_2^EK_3^S)}{K_3^EK_2^H-K_2^EK_3^H},\quad Z_4=-\frac{+(G_2K_3^E-G_3K_2^E)}{K_3^EK_2^H-K_2^EK_3^H}$$

Placing Eq. (68) in the first relation of Eq. (53) results in

$$K^*\widetilde{W}+G_1\widetilde{W}^3+Z^*\widetilde{W}^2+\Psi_1W^*=0 \qquad (69)$$

where

$$K^*=K_1^S+K_1^EZ_1+K_1^HZ_3$$
$$Z^*=K_1^EZ_2+K_1^HZ_4+Q_1 \qquad (70)$$

Solving Eq. (69) gives the buckling temperatures as functions of buckling deflection $\widetilde{W}$.

5. Numerical results and discussions

Discussions on nonlinear stability behavior of elastic nanobeams with MEE layers having geometrical imperfection have been presented in this chapter. The nanobeam's length has been selected as L = 10 nm. Due to the reason that there is no published study about buckling of geometrically imperfect sandwich nano-size beams with MEE layers, the buckling loads have been verified with those for perfect elastic nano-size beams with piezoelectric and magnetic field effects. Table 2 represents the nonlinear buckling loads of a nano-dimension beam according to diverse values for nonlocal parameter comparing to those presented by Li *et al.* (2016). It is obvious that presented result is identically the same as that provided by Li *et al.* (2016). So, the presented methodology can accurately predict buckling behavior of smart nanobeams under magneto-electrical fields.

Fig. 2 illustrates the post-buckling curves of a sandwich nano-size beam for various nonlocal parameters with and without geometric imperfection effects. In this figure, the piezoelectric phase percentage is set to V_f = 20%; applied electric voltage and magnetic potential are simply considered as V_E = 0, Ω = 0. For the sandwich beam, the thickness of layers is assumed as h_p = 0.1 h. One can express that increasing in the magnitude of dimensionless deflection yields larger buckling temperature for a perfect nanobeam due to hardening effects raised from geometric nonlinearity. For both perfect and imperfect sandwich

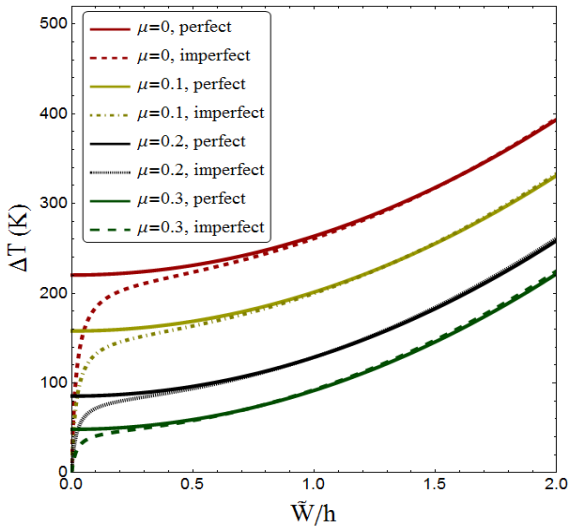

Fig. 2 Post-buckling temperature versus normalized deflection of sandwich nano-size beam for various nonlocal parameters (V_f = 20%, V_E = 0, Ω = 0, L/h = 50, h_p = 0.1 h)

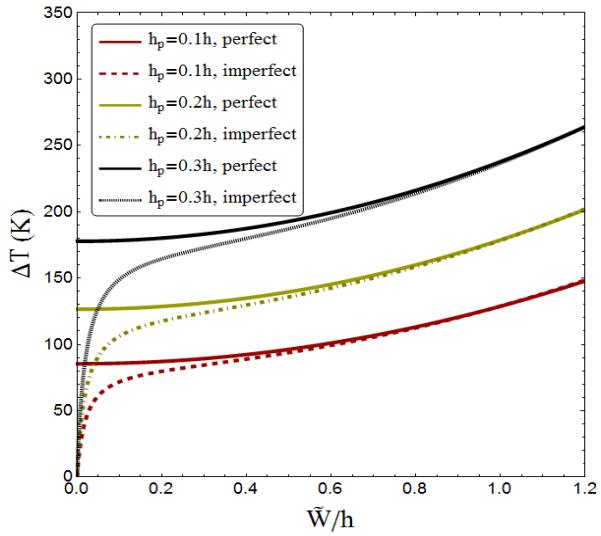

Fig. 3 Post-buckling temperature versus normalized deflection of sandwich nano-size beam for various piezo-magnetic thicknesses (V_f = 20%, V_E = 0, Ω = 0, μ = 0.2, L/h = 50, W*/h = 0.02)

nanobeams, increase of nonlocal parameter yields smaller buckling temperature since the total stiffness of the nanobeam is reduced. So, nonlocal stress field which captures long range atomic interaction has a great influence on buckling characteristics of geometrically imperfect sandwich nanobeams with two MEE layers.

Illustrated in Fig. 3 is the influence of layers thickness on post-buckling curves of a sandwich nanobeam modeled by nonlocal theory (μ = 0.2). This graph is presented based on perfect and imperfect sandwich nanobeams. It is obvious that increasing in the thickness of layers (h_p) results in greater buckling loads. So, it can be concluded that the buckling characteristics of a nano-size sandwich beam can be improved by enlarging the thickness of its layers.

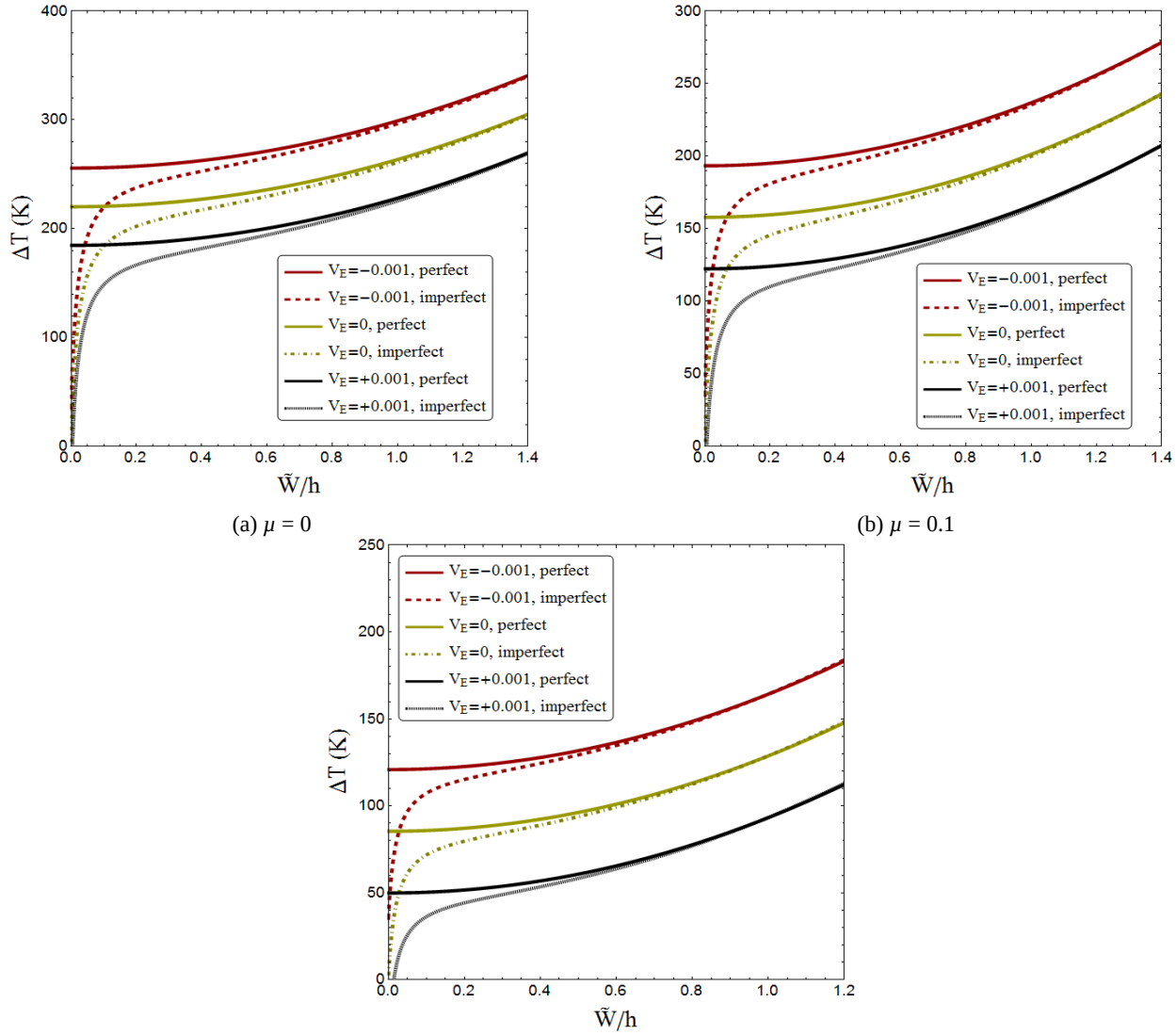

(a) μ = 0 (b) μ = 0.1

(c) μ = 0.2

Fig. 4 Post-buckling temperature versus normalized deflection of sandwich nano-size beam for various electric voltages (h_p = 0.1 h, V_f = 20%, W*/h = 0.02, Ω = 0)

Assuming various values for nonlocal parameter, Figs. 4 and 5 respectively show the influences of applied electrical voltages (V_E) and magnetic potential (Ω) on post-buckling curves of a sandwich nano-scale beam with/without geometric imperfections effects. The piezoelectric constituent volume has been considered as V_f = 20%. One can see that applying negative electrical voltages to a nano-scale beam causes greater nonlinear buckling temperature than applying a positive electrical voltage. Such observation is because of raised compressive loads by positive electrical voltages. Such compressive loads may result in the decrement in structural stiffness of the nano-scale beam as well as buckling temperature. Another observation is that the effect of magnetic potential on buckling temperature is in contrast to electrical voltages. Actually, negative magnetic potentials yield smaller buckling temperature than a positive one. Such observations are valid for both perfect and imperfect nano-scale beams having MEE layers.

Fig. 6 shows the effect of geometric imperfection amplitude (W*/h) on thermal post-buckling curves of smart nanobeam having piezoelectric phase percentage of V_f = 20%. It is assumed that the nanobeam is exposed to an electric voltage of V_E = 0. It is seen from the figure that increasing geometric imperfection amplitude may reduce the magnitude of buckling temperature at small ranges of normalized deflection. This is related to the energy stored in an imperfect nanobeam. However, an imperfect nanobeam has no critical bucking. Again, it can be observed that the nonlinear buckling characteristics of a smart nanobeam having geometrical imperfection largely depend on the buckling amplitude. Actually, at larger values of normalized deflection, the influence of geometric imperfection on buckling curves become negligible.

Fig. 7 shows the variation of buckling temperature of a sandwich nano-scale beam having MEE layers versus exerted electrical voltages (V_E) according to diverse values

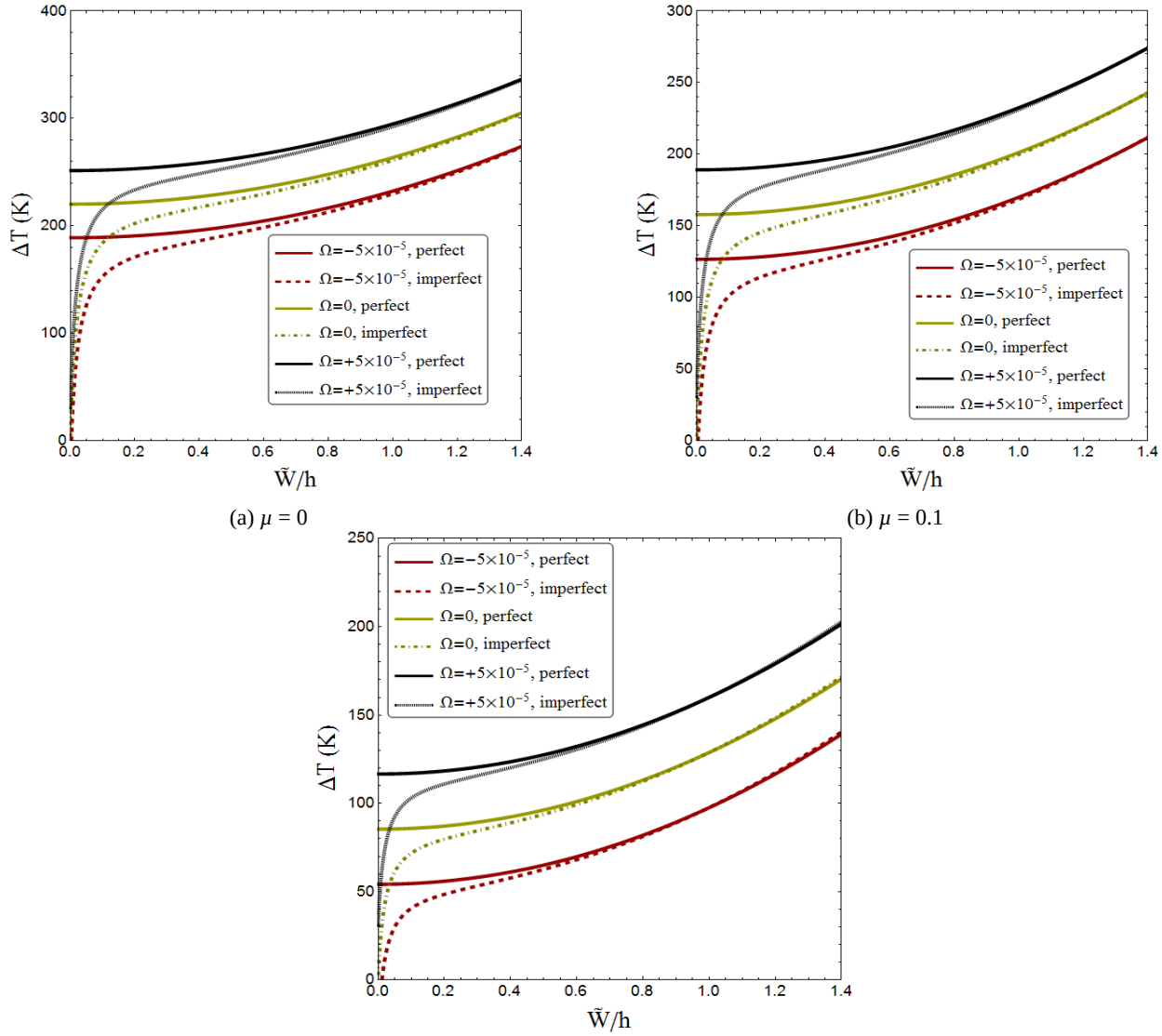

(a) μ = 0

(b) μ = 0.1

(c) μ = 0.2

Fig. 5 Post-buckling temperature versus normalized deflection of sandwich nano-size beam for various magnetic potentials (h_p = 0.1 h, V_f = 20%, W*/h = 0.02, V_E = 0)

for piezoelectric constituent volume (V_f). The geometrical imperfection magnitude and dimensionless vibration amplitude are respectively considered as W*/h = 0 and $\tilde{W}$/h = 0.5. One may see that the buckling temperature stay constant by varying in electrical voltages at V_f = 0%. Thus, the nanobeam buckling is not dependent to electric voltages at zero volume of piezoelectric constituent. According to different values for V_f, varying the values of electrical voltages from negative to positive results in decrement in value of buckling temperatures. The main conclusion from the figure is that the buckling temperature reduces via higher rates by increase of piezoelectric constituent volume. Thus, by increase of piezoelectric constituent volume the sandwich nanobeams become more susceptible to exerted electrical voltages.

6. Conclusions

Nonlinear thermal stability behavior of elastic nanobeams with MEE layers having geometrical imperfection were studied in this article. Nonlocal theory was employed for mathematical formulating of the sandwich nanobeam. An analytical trend was proposed to derive post-buckling curves of the sandwich nanobeam. According to different values for V_f, varying the values of electrical voltages from negative to positive led to decrement in value of buckling temperatures. The main conclusion was that the buckling temperature reduced via higher rates by increase of piezoelectric constituent volume. Another observation was that the effect of magnetic potential on buckling temperature is in contrast to electrical voltages. Actually, negative magnetic potentials yield smaller buckling temperature than a positive one. It was found that increasing in the thickness of layers results in

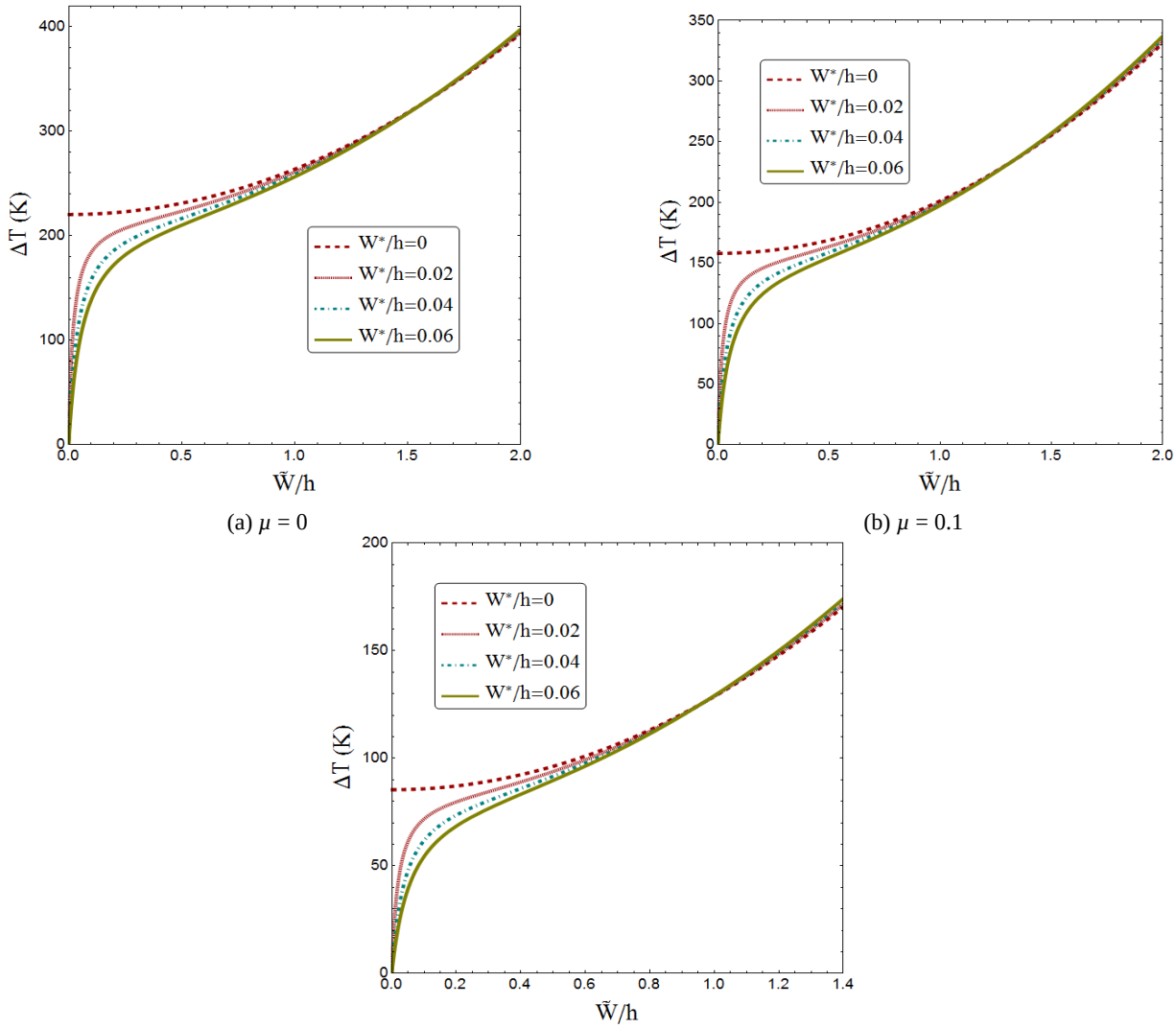

(a) $\mu = 0$ (b) $\mu = 0.1$

(c) $\mu = 0.2$

Fig. 6 Post-buckling temperature versus normalized deflection of sandwich nano-size beam for various geometric imperfections (h_p = 0.1 h, V_f = 20%, L/h = 50, V_E = 0)

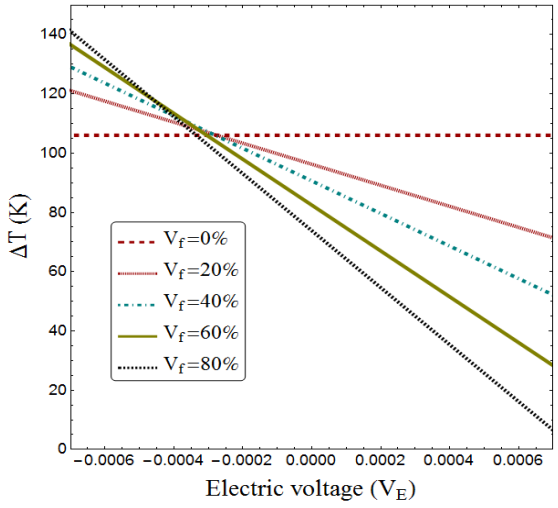

Fig. 7 Post-buckling temperature versus electric voltage of the nanobeam for various piezoelectric volume fractions (h_p = 0.1 h, L/h = 50, W/h = 0.5, W*/h = 0, Ω = 0, μ = 0.2)

greater buckling temperature. So, it can be concluded that the buckling characteristics of a nano-size sandwich beam can be improved by enlarging the thickness of its layers.

Acknowledgments

The authors would like to thank Mustansiriyah university (www.uomustansiriyah.edu.iq) Baghdad-Iraq for its support in the present work.

References

Aboudi, J. (2001), "Micromechanical analysis of fully coupled electro-magneto-thermo-elastic multiphase composites", *Smart Mater. Struct.*, **10**(5), 867. https://doi.org/10.1088/0964-1726/10/5/303

Ahmed, R.A., Fenjan, R.M. and Faleh, N.M. (2019), "Analyzing post-buckling behavior of continuously graded FG nanobeams with geometrical imperfections", *Geomech. Eng., Int. J.*, **17**(2), 175-180. https://doi.org/10.12989/gae.2019.17.2.175

Akbaş, Ş.D. (2016), "Forced vibration analysis of viscoelastic nanobeams embedded in an elastic medium", *Smart Struct. Syst., Int. J.*, **18**(6), 1125-1143. http://dx.doi.org/10.12989/sss.2016.18.6.1125

Allam, M.N.M., Tantawy, R. and Zenkour, A.M. (2018), "Magneto-thermo-elastic response of exponentially graded piezoelectric hollow spheres", *Adv. Computat. Des., Int. J.*, **3**(3), 303-318. https://doi.org/10.12989/acd.2018.3.3.303

Al-Maliki, A.F., Faleh, N.M. and Alasadi, A.A. (2019), "Finite element formulation and vibration of nonlocal refined metal foam beams with symmetric and non-symmetric porosities", *Struct. Monitor. Mainten.*, **6**(2), 147-159. https:// doi.org/10.12989/smm.2019.6.2.147

Annigeri, A.R., Ganesan, N. and Swarnamani, S. (2007), "Free vibration behaviour of multiphase and layered magneto-electro-elastic beam", *J. Sound Vib.*, **299**(1-2), 44-63. https://doi.org/10.1016/j.jsv.2006.06.044

Azimi, M., Mirjavadi, S.S., Shafiei, N. and Hamouda, A.M.S. (2017), "Thermo-mechanical vibration of rotating axially functionally graded nonlocal Timoshenko beam", *Appl. Phys. A*, **123**(1), 104. https://doi.org/10.1007/s00339-016-0712-5

Azimi, M., Mirjavadi, S.S., Shafiei, N., Hamouda, A.M.S. and Davari, E. (2018), "Vibration of rotating functionally graded Timoshenko nano-beams with nonlinear thermal distribution", *Mech. Adv. Mater. Struct.*, **25**(6), 467-480. https://doi.org/10.1080/15376494.2017.1285455

Barati, M.R. (2017), "Coupled effects of electrical polarization-strain gradient on vibration behavior of double-layered flexoelectric nanoplates", *Smart Struct. Syst., Int. J.*, **20**(5), 573-581. https://doi.org/10.12989/sss.2017.20.5.573

Behera, S. and Kumari, P. (2018), "Free vibration of Levy-type rectangular laminated plates using efficient zig-zag theory", *Adv. Computat. Des., Int. J.*, **3**(3), 213-232. https://doi.org/10.12989/acd.2018.3.3.213

Bensattalah, T., Zidour, M. and Daouadji, T.H. (2018), "Analytical analysis for the forced vibration of CNT surrounding elastic medium including thermal effect using nonlocal Euler-Bernoulli theory", *Adv. Mater. Res., Int. J.*, **7**(3), 163-174. https://doi.org/10.12989/amr.2018.7.3.163

Besseghier, A., Houari, M.S.A., Tounsi, A. and Mahmoud, S.R. (2017), "Free vibration analysis of embedded nanosize FG plates using a new nonlocal trigonometric shear deformation theory", *Smart Struct. Syst., Int. J.*, **19**(6), 601-614. https://doi.org/10.12989/sss.2017.19.6.601

Bounouara, F., Benrahou, K.H., Belkorissat, I. and Tounsi, A. (2016), "A nonlocal zeroth-order shear deformation theory for free vibration of functionally graded nanoscale plates resting on elastic foundation", *Steel Compos. Struct., Int. J.*, **20**(2), 227-249. https://doi.org/10.12989/scs.2016.20.2.227

Chaudhary, S., Sahu, S.A. and Singhal, A. (2017), "Analytic model for Rayleigh wave propagation in piezoelectric layer overlaid orthotropic substratum", *Acta Mechanica*, **228**(2), 495-529. https://doi.org/10.1007/s00707-016-1708-0

Chaudhary, S., Sahu, S.A. and Singhal, A. (2018), "On secular equation of SH waves propagating in pre-stressed and rotating piezo-composite structure with imperfect interface", *J. Intel. Mater. Syst. Struct.*, **29**(10), 2223-2235. https://doi.org/10.1177%2F1045389X18758192

Chaudhary, S., Sahu, S.A., Dewangan, N. and Singhal, A. (2019a), "Stresses produced due to moving load in a prestressed piezoelectric substrate", *Mech. Adv. Mater. Struct.*, **26**(12), 1028-1041. https://doi.org/10.1080/15376494.2018.1430265

Chaudhary, S., Sahu, S., Singhal, A. and Nirwal, S. (2019b), "Interfacial imperfection study in pres-stressed rotating multiferroic cylindrical tube with wave vibration analytical approach", *Mater. Res. Express*, **6**(10), 105704. https://doi.org/10.1088/2053-1591/ab3880

Eltaher, M.A., Emam, S.A. and Mahmoud, F.F. (2012), "Free vibration analysis of functionally graded size-dependent nanobeams", *Appl. Mathe. Computat.*, **218**(14), 7406-7420. https://doi.org/10.1016/j.amc.2011.12.090

Eshraghi, I., Jalali, S.K. and Pugno, N.M. (2016), "Imperfection sensitivity of nonlinear vibration of curved single-walled carbon nanotubes based on nonlocal timoshenko beam theory", *Materials*, **9**(9), 786. https://doi.org/10.3390/ma9090786

Eringen, A.C. (1972), "Linear theory of nonlocal elasticity and dispersion of plane waves", *Int. J. Eng. Sci.*, **10**(5), 425-435. https://doi.org/10.1016/0020-7225(72)90050-X

Fenjan, R.M., Ahmed, R.A., Alasadi, A.A. and Faleh, N.M. (2019), "Nonlocal strain gradient thermal vibration analysis of double-coupled metal foam plate system with uniform and non-uniform porosities", *Coupl. Syst. Mech., Int. J.*, **8**(3), 247-257. https://doi.org/10.12989/csm.2019.8.3.247

Guo, J., Chen, J. and Pan, E. (2016), "Static deformation of anisotropic layered magnetoelectroelastic plates based on modified couple-stress theory", *Compos. Part B: Eng.*, **107**, 84-96. https://doi.org/10.1016/j.compositesb.2016.09.044

Jandaghian, A.A. and Rahmani, O. (2016), "Free vibration analysis of magneto-electro-thermo-elastic nanobeams resting on a Pasternak foundation", *Smart Mater. Struct.*, **25**(3), 035023. https://doi.org/10.1088/0964-1726/25/3/035023

Ke, L.L. and Wang, Y.S. (2014), "Free vibration of size-dependent magneto-electro-elastic nanobeams based on the nonlocal theory", *Physica E: Low-Dimens. Syst. Nanostruct.*, **63**, 52-61. https://doi.org/10.1016/j.physe.2014.05.002

Kumaravel, A., Ganesan, N. and Sethuraman, R. (2007), "Buckling and vibration analysis of layered and multiphase magneto-electro-elastic beam under thermal environment", *Multidiscipl. Model. Mater. Struct.*, **3**(4), 461-476. https://doi.org/10.1163/157361107782106401

Li, Y. and Shi, Z. (2009), "Free vibration of a functionally graded piezoelectric beam via state-space based differential quadrature", *Compos. Struct.*, **87**(3), 257-264. https://doi.org/10.1016/j.compstruct.2008.01.012

Li, Y.S., Ma, P. and Wang, W. (2016), "Bending, buckling, and free vibration of magnetoelectroelastic nanobeam based on nonlocal theory", *J. Intel. Mater. Syst. Struct.*, **27**(9), 1139-1149. https://doi.org/10.1177%2F1045389X15585899

Li, L., Tang, H. and Hu, Y. (2018), "Size-dependent nonlinear vibration of beam-type porous materials with an initial geometrical curvature", *Compos. Struct.*, **184**, 1177-1188. https://doi.org/10.1016/j.compstruct.2017.10.052

Mirjavadi, S.S., Rabby, S., Shafiei, N., Afshari, B.M. and Kazemi, M. (2017a), "On size-dependent free vibration and thermal buckling of axially functionally graded nanobeams in thermal environment", *Appl. Phys. A*, **123**(5), 315. https://doi.org/10.1007/s00339-017-0918-1

Mirjavadi, S.S., Afshari, B.M., Shafiei, N., Hamouda, A.M.S. and Kazemi, M. (2017b), "Thermal vibration of two-dimensional functionally graded (2D-FG) porous Timoshenko nanobeams. *Steel Compos. Struct., Int. J.*, **25**(4), 415-426. https://doi.org/10.12989/scs.2017.25.4.415

Mirjavadi, S.S., Afshari, B.M., Barati, M.R. and Hamouda, A.M.S. (2018a), "Strain gradient based dynamic response analysis of heterogeneous cylindrical microshells with porosities under a moving load", *Mater. Res. Express*, **6**(3), 035029. https://doi.org/10.1088/2053-1591/aaf5a2

Mirjavadi, S.S., Afshari, B.M., Khezel, M., Shafiei, N., Rabby, S. and Kordnejad, M. (2018b), "Nonlinear vibration and buckling of functionally graded porous nanoscaled beams", *J. Brazil. Soc. Mech. Sci. Eng.*, **40**(7), 352. https://doi.org/10.1007/s40430-018-1272-8

Mirjavadi, S.S., Forsat, M., Hamouda, A.M.S. and Barati, M.R. (2019a), "Dynamic response of functionally graded graphene

nanoplatelet reinforced shells with porosity distributions under transverse dynamic loads", *Mater. Res. Express*, **6**(7), 075045. https://doi.org/10.1088/2053-1591/ab1552

Mirjavadi, S.S., Forsat, M., Nikookar, M., Barati, M.R. and Hamouda, A.M.S. (2019b), "Nonlinear forced vibrations of sandwich smart nanobeams with two-phase piezo-magnetic face sheets", *Eur. Phys. J. Plus*, **134**(10), 508. https://doi.org/10.1140/epjp/i2019-12806-8

Mirjavadi, S.S., Afshari, B.M., Barati, M.R. and Hamouda, A.M. S. (2019c), "Transient response of porous FG nanoplates subjected to various pulse loads based on nonlocal stress-strain gradient theory", *Eur. J. Mech.-A/Solids*, **74**, 210-220. https://doi.org/10.1016/j.euromechsol.2018.11.004

Mirjavadi, S.S., Afshari, B.M., Barati, M.R. and Hamouda, A.M.S. (2019d), "Nonlinear free and forced vibrations of graphene nanoplatelet reinforced microbeams with geometrical imperfection", *Microsyst. Technol.*, **25**, 3137-3150. https://doi.org/10.1007/s00542-018-4277-4

Mirjavadi, SS., Forsat, M., Barati, M.R., Abdella, G.M., Hamouda, A.M.S., Afshari, B.M. and Rabby, S. (2019e), "Post-buckling analysis of piezo-magnetic nanobeams with geometrical imperfection and different piezoelectric contents", *Microsyst. Technol.*, **25**(9), 3477-3488. https://doi.org/10.1007/s00542-018-4241-3

Mirjavadi, S.S., Forsat, M., Barati, M.R., Abdella, G.M., Afshari, B.M., Hamouda, A.M.S. and Rabby, S. (2019f), "Dynamic response of metal foam FG porous cylindrical micro-shells due to moving loads with strain gradient size-dependency", *Eur. Phys. J. Plus*, **134**(5), 214. https://doi.org/10.1140/epjp/i2019-12540-3

Mohammadi, H., Mahzoon, M., Mohammadi, M. and Mohammadi, M. (2014), "Postbuckling instability of nonlinear nanobeam with geometric imperfection embedded in elastic foundation", *Nonlinear Dyn.*, **76**(4), 2005-2016. https://doi.org/10.1007/s11071-014-1264-x

Mohammadimehr, M. and Alimirzaei, S. (2016), "Nonlinear static and vibration analysis of Euler-Bernoulli composite beam model reinforced by FG-SWCNT with initial geometrical imperfection using FEM", *Struct. Eng. Mech., Int. J.*, **59**(3), 431-454. http://dx.doi.org/10.12989/sem.2016.59.3.431

Mouffoki, A., Bedia, E.A., Houari, M.S.A., Tounsi, A. and Mahmoud, S.R. (2017), "Vibration analysis of nonlocal advanced nanobeams in hygro-thermal environment using a new two-unknown trigonometric shear deformation beam theory. *Smart Struct. Syst., Int. J.*, **20**(3), 369-383. https://doi.org/10.12989/sss.2017.19.2.115

Mu'tasim, S., Al-Qaisia, A.A. and Shatarat, N.K. (2017), "Nonlinear Vibrations of a SWCNT with Geometrical Imperfection Using Nonlocal Elasticity Theory", *Modern Appl. Sci.*, **11**(10), 91. https://doi.org/10.5539/mas.v11n10p91

Nan, C.W. (1994), "Magnetoelectric effect in composites of piezoelectric and piezomagnetic phases", *Phys. Rev. B*, **50**(9), 6082. https://doi.org/10.1103/PhysRevB.50.6082

Nirwal, S., Sahu, S.A., Singhal, A. and Baroi, J. (2019), "Analysis of different boundary types on wave velocity in bedded piezo-structure with flexoelectric effect", *Compos. Part B: Eng.*, **167**, 434-447. https://doi.org/10.1016/j.compositesb.2019.03.014

Pan, E. and Han, F. (2005), "Exact solution for functionally graded and layered magneto-electro-elastic plates", *Int. J. Eng. Sci.*, **43**(3-4), 321-339. https://doi.org/10.1016/j.ijengsci.2004.09.006

Sahu, S.A., Singhal, A. and Chaudhary, S. (2018), "Surface wave propagation in functionally graded piezoelectric material: an analytical solution", *J. Intel. Mater. Syst. Struct.*, **29**(3), 423-437. https://doi.org/10.1177%2F1045389X17708047

Singh, M.K., Sahu, S.A., Singhal, A. and Chaudhary, S. (2018), "Approximation of surface wave velocity in smart composite structure using Wentzel–Kramers–Brillouin method", *J. Intel. Mater. Syst. Struct.*, **29**(18), 3582-3597. https://doi.org/10.1177%2F1045389X18786464

Singhal, A. and Chaudhary, S. (2019), "Mechanics of 2D Elastic Stress Waves Propagation Impacted by Concentrated Point Source Disturbance in Composite Material Bars", *J. Appl. Computat. Mech.* https://doi.org/10.22055/JACM.2019.29666.1621

Singhal, A. and Sahu, S.A. (2017), "Transference of rayleigh waves in corrugated orthotropic layer over a pre-stressed orthotropic half-space with self weight", *Procedia Eng.*, **173**, 972-979. https://doi.org/10.1016/j.proeng.2016.12.164

Singhal, A., Sahu, S.A. and Chaudhary, S. (2018a), "Approximation of surface wave frequency in piezo-composite structure", *Compos. Part B: Eng.*, **144**, 19-28. https://doi.org/10.1016/j.compositesb.2018.01.017

Singhal, A., Sahu, S.A. and Chaudhary, S. (2018b), "Liouville-Green approximation: An analytical approach to study the elastic waves vibrations in composite structure of piezo material", *Compos. Struct.*, **184**, 714-727. https://doi.org/10.1016/j.compstruct.2017.10.031

Singhal, A., Sahu, S.A. and Chaudhary, S. (2019a), "Study of surface wave vibration in rotating human long bones of cylindrical shape under the magnetic field influence", *Waves Random Complex Media*, 1-17. https://doi.org/10.1080/17455030.2019.1686551

Singhal, A., Sahu, S.A., Chaudhary, S. and Baroi, J. (2019b), "Initial and couple stress influence on the surface waves transmission in material layers with imperfect interface", *Mater. Res. Express*, **6**(10), 105713. https://doi.org/10.1088/2053-1591/ab40e2

Thai, H.T. and Vo, T.P. (2012), "A nonlocal sinusoidal shear deformation beam theory with application to bending, buckling, and vibration of nanobeams", *Int. J. Eng. Sci.*, **54**, 58-66. https://doi.org/10.1016/j.ijengsci.2012.01.009

Zemri, A., Houari, M.S.A., Bousahla, A.A. and Tounsi, A. (2015), "A mechanical response of functionally graded nanoscale beam: an assessment of a refined nonlocal shear deformation theory beam theory", *Struct. Eng. Mech., Int. J.*, **54**(4), 693-710. https://doi.org/10.12989/sem.2015.54.4.693

CC